

Electronic Supplementary Information

Extending the high-performing boundaries of fully bio-based thermal shrinkage film targeted for food packaging applications

A-Yeon Lim,^{a,b,†} Sung bae Park,^{a,†} Yumi Choi,^{a,b} Dongyeop X. Oh,^{a,c,d,*} Jeyoung Park,^{a,e,*}
Hyeonyeol Jeon,^{a,c,*} and Jun Mo Koo^{f,*}

*^aResearch Center for Bio-based Chemistry, Korea Research Institute of Chemical
Technology (KRICT), Ulsan 44429, Republic of Korea. E-mail: dongyeop@kRICT.re.kr,
hyjeon@kRICT.re.kr*

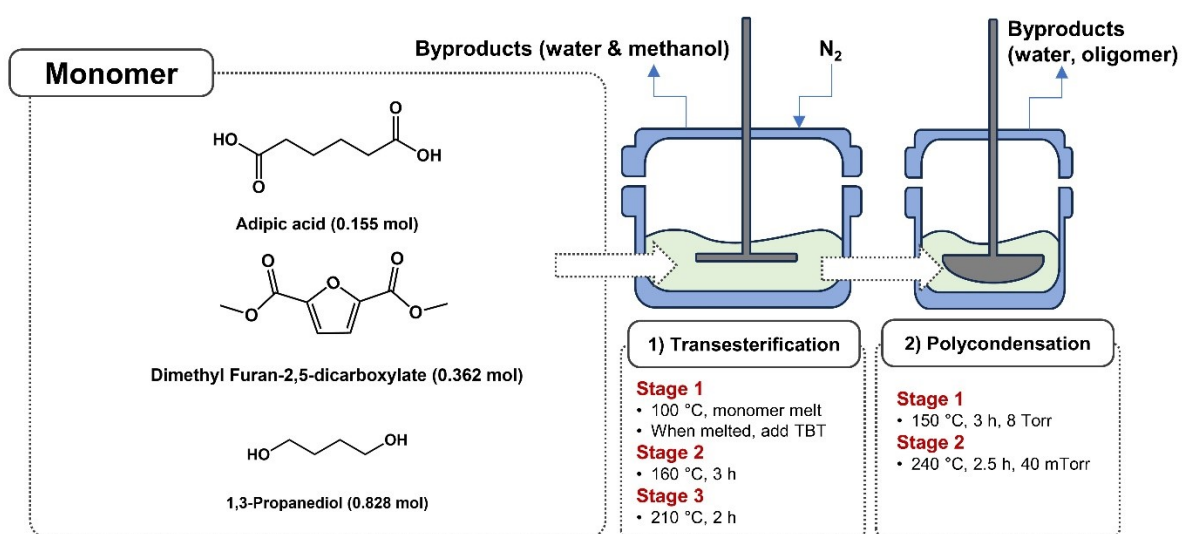
*^bSchool of Chemical Engineering, Pusan National University (PNU), Busan 46421, Republic
of Korea.*

*^cAdvanced Materials and Chemical Engineering, University of Science and Technology
(UST), Daejeon 34113, Republic of Korea.*

*^dDepartment of Polymer Science and Engineering and Program in Environmental and
Polymer Engineering, Inha University, Incheon 22212, Republic of Korea. E-mail:
d.oh@inha.ac.kr*

*^eDepartment of Chemical and Biomolecular Engineering, Sogang University, Seoul 04107,
Republic of Korea. E-mail: jeypark@sogang.ac.kr*

*^fDepartment of Organic Materials Engineering, Chungnam National University, Daejeon
34134, Republic of Korea. E-mail: junmokoo@cnu.ac.kr*



Scheme S1. Schematics of synthesis steps including transesterification and polycondensation.

Table S1. Characteristic properties of PPAFs polymerized with various feed ratios

Sample code	Feed ratio (Aro : Ali : PDO) ^a	PF / PA ^b (mol %)	M _n (g mol ⁻¹)	M _w (g mol ⁻¹)	PDI
PPAF 90	9 : 1 : 16	-	-	-	-
PPAF 80	8 : 2 : 16	80.1 / 19.9	34000	45000	1.32
PPAF 70	7 : 3 : 16	68.2 / 31.8	36000	47000	1.30
PPAF 60	6 : 4 : 16	58.2 / 41.8	31000	41000	1.34
PPAF 50	5 : 5 : 16	50.7 / 49.3	42500	53400	1.25

^a : Aro. is DMFD as aromatic acidic monomer, and Ali. is AA as aliphatic acidic monomer.

^b : The composition ratio of Furan-2,5-dicarboxylate and Adipic acid

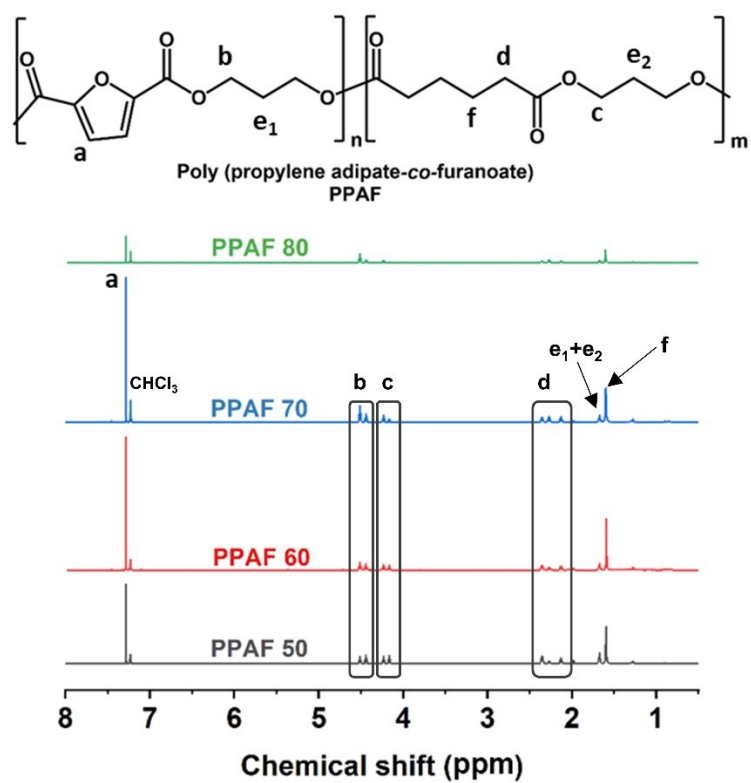


Figure S1. ¹H NMR spectra of PPAF copolyesters with various aromatic contents.

Cycle	Strain (%)*			
	250	200	150	100
1	46.8	44.4	48.1	46.8
2	38.5	51.8	48.8	34.5
3	34.5	48.0	42.0	38.2
4	38.2	45.4	40.5	44.5
5	44.6	47.1	48.2	43.6
6	43.6	53.0	49.3	47.9
7	47.8	53.0	55.9	40.2
8	40.2	55.4	50.4	34.5
9	34.5	54.1	44.5	38.5
10	38.5	53.0	42.4	38.5

Table S2. Hysteresis data for PPAF 70 at specific strains

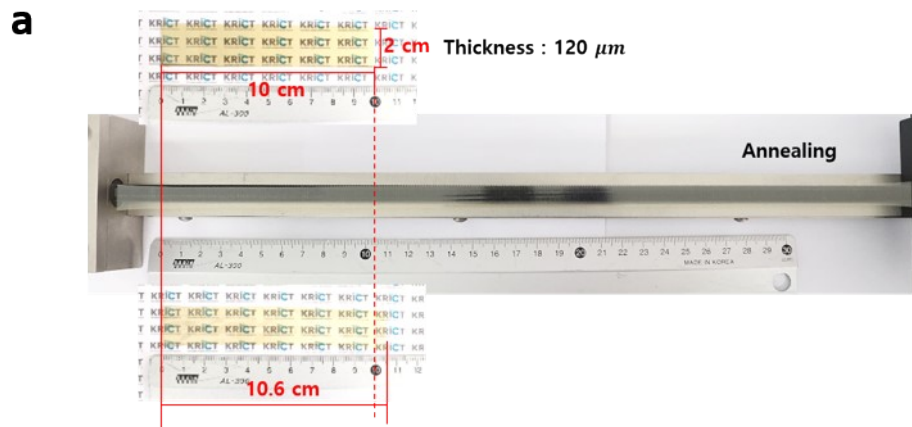
* Recovery position according to the cycle for each strain. It is a position that contracts according to the cycle when pulled by each strain, and usually the position must increase as the cycle increases, but due to the structural specificity of PPAF 70, it shows a random position without a constant tendency.



Figure S2. (a) Stress–strain curves for PPAT 70. (b) No change after elongation at break.

Table S3. Mechanical properties of PPAT 70

	Young's modulus (MPa)	Tensile Strength (MPa)	Elongation at break (%)	Toughness (MJ m ⁻³)
1	1040.2	27.9	293.7	52.4
2	950.2	27.9	284.5	50.1
3	821.9	27.6	284.5	48.8
Average	915.7	27.8	287.6	50.4



b

$$\text{Recovery rate (\%)} = \frac{L_i}{L_f} \times 100$$

L_i : Initial sample length
 L_f : Final sample length after shrinkage

Figure S3. (a) Annealing when elongated by 600%, and recovery with a heating gun. (b) Equation of recovery rate.

Table S4. PPAF 70 recovery rate according to annealing time.

Annealing time (h)	Strain (%)	Heating Temperature (°C)	Recover length (cm)	Recovery rate (%)	Thickness (μm)
1			10.6	94.3	
3	600	100	11.5	87.0	120
5			12.2	82.0	

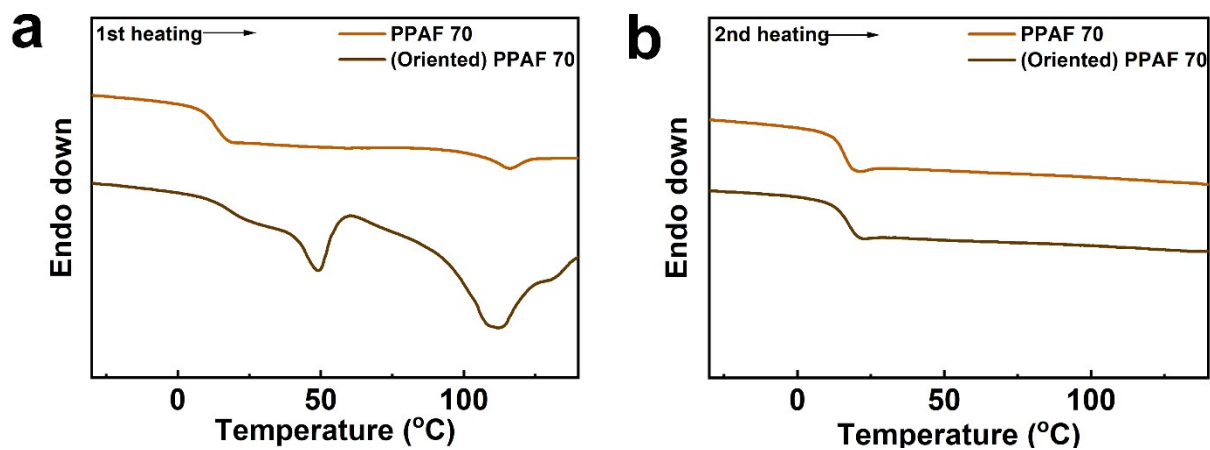


Figure. S4. DSC (a) 1st (b) 2nd heating curve of PPAF70 with neat and oriented sample.

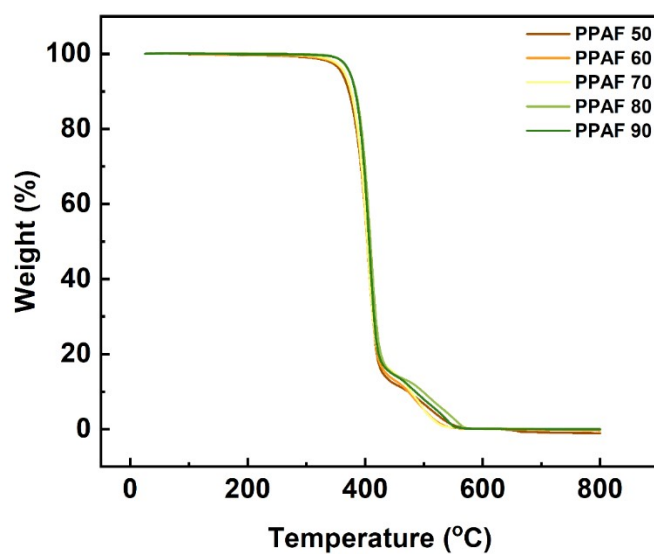


Figure S5. TGA curve of series of PPAFs under N₂ atmosphere.

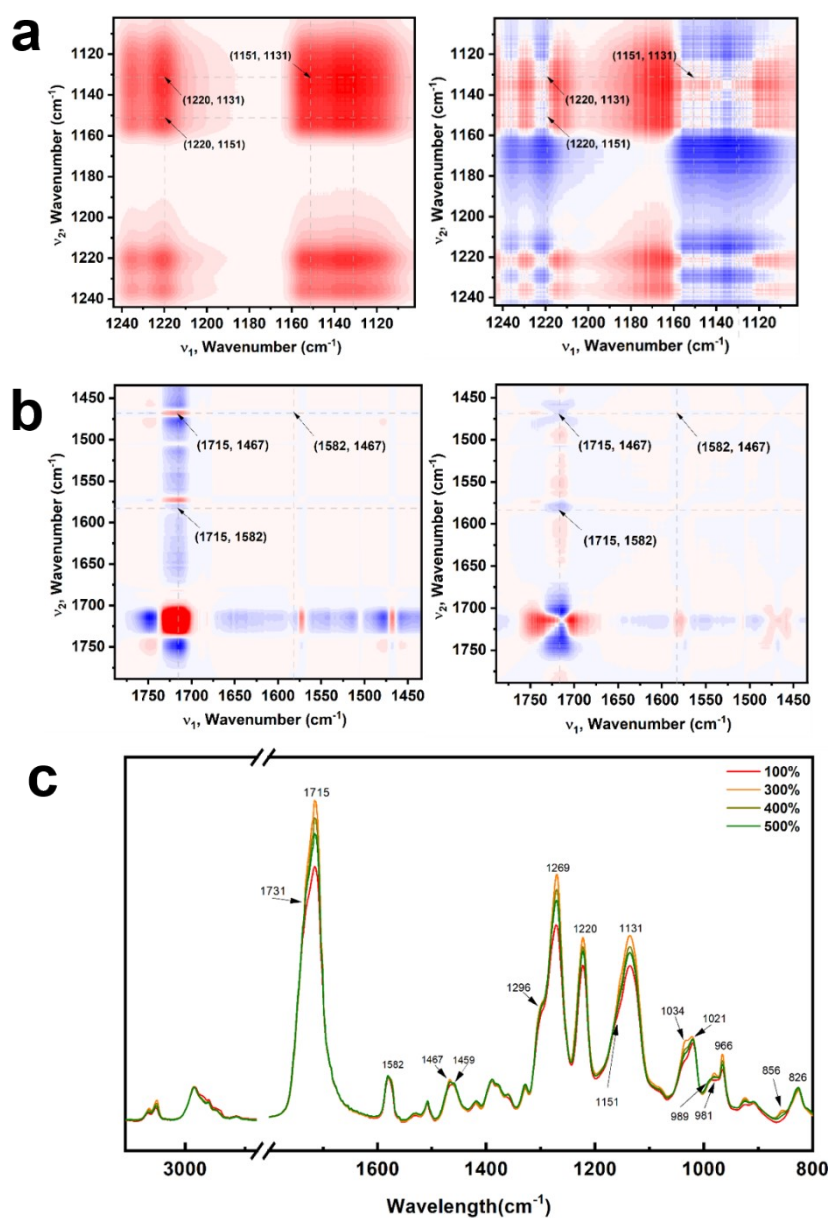
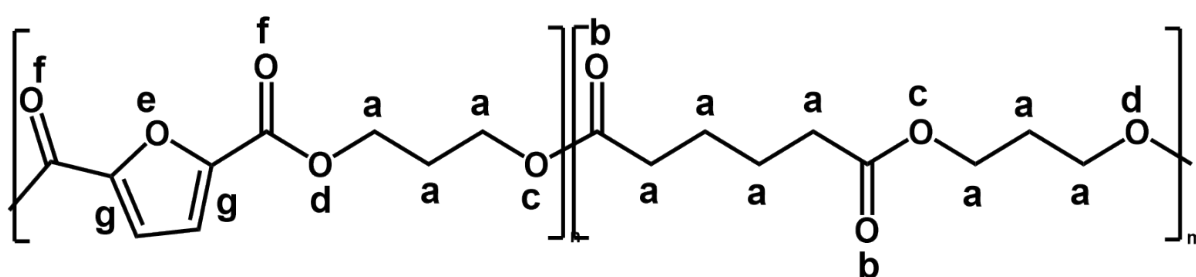


Figure S6. (a) Synchronous (left) and asynchronous (right) homogeneous 2DCOS spectra in the 1243–1102 cm⁻¹ range. (b) Synchronous (left) and asynchronous (right) homogeneous 2DCOS spectra in the 1788–1434 cm⁻¹ range (c) One dimensional FT-IR spectra of PPAF 70 when elongated between 300 and 500%.

Table S5. 2DCOS analysis of PPAF 70 when elongated between 300 and 500%, and

Sequential order	Wavenumber (cm ⁻¹)	Intensity change	Assignment
a	1467	▼	-CH ₂ - bending
b	1731	▼	C=O from aliphatic segment
c	1151	▼	C-O stretching
d	1131	▼	C-O stretching
e	1220	▼	=C-O-C= furan ring vibration
f	1715	▼	C=O adjacent to furan ring
g	1582	▲	C=C furan ring stretching

corresponding sequences and intensity changes.



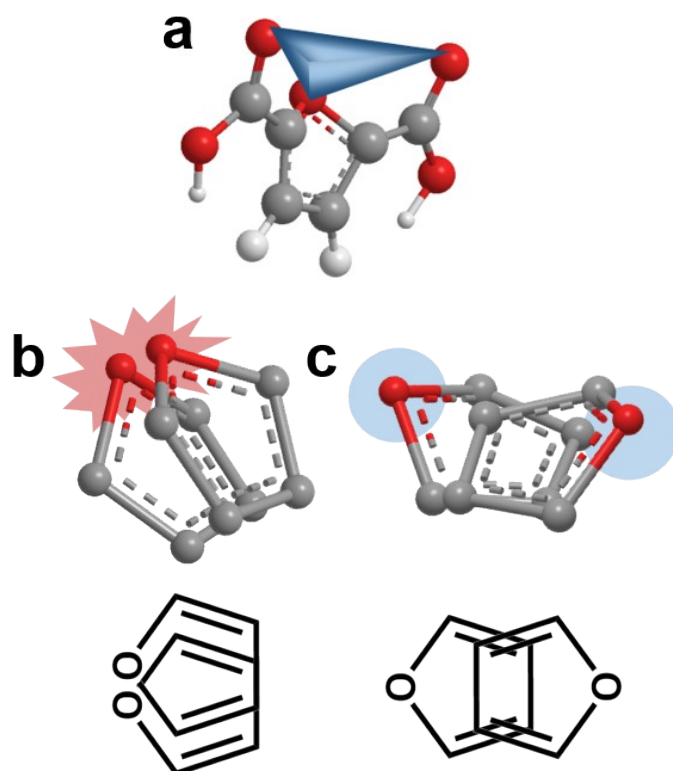


Figure S7. (a) Molecular structure of distorted FDCA. (b) Wrongly stacked furan rings: 3D (upper) and 2D (lower). (c) Correctly stacked furan rings: 3D (upper) and 2D (lower).

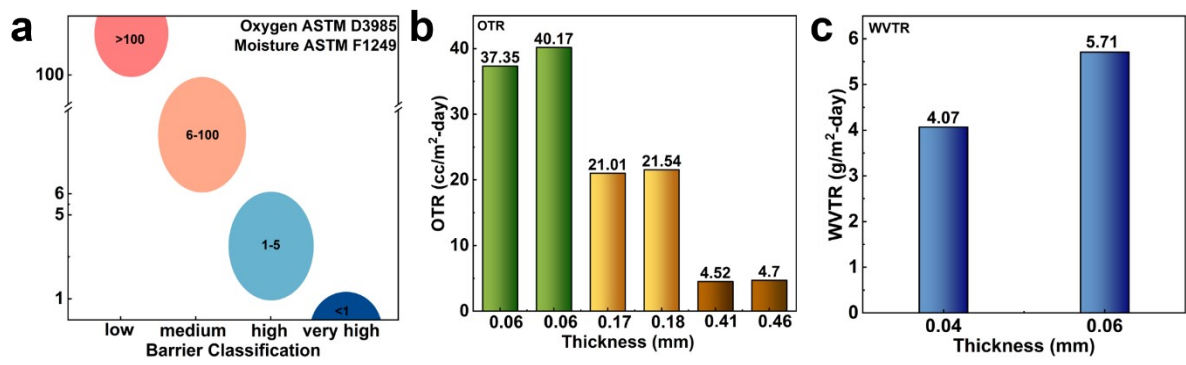


Figure S8. (a) Standard OTR and WVTR barrier classification values (ASTM D3985, ASTM F1249) (b) OTR value, and (c) WVTR value of PPAF 70 according to sample thickness.

Movie S1.